

Intra-beam scattering for free electron lasers and its modeling in chicanes

G. Penn

Center for Beam Physics, Lawrence Berkeley National Laboratory,
Berkeley, CA 94720, USA

August 2014

Disclaimer

This document was prepared as an account of work sponsored by the United States Government. While this document is believed to contain correct information, neither the United States Government nor any agency thereof, nor The Regents of the University of California, nor any of their employees, makes any warranty, express or implied, or assumes any legal responsibility for the accuracy, completeness, or usefulness of any information, apparatus, product, or process disclosed, or represents that its use would not infringe privately owned rights. Reference herein to any specific commercial product, process, or service by its trade name, trademark, manufacturer, or otherwise, does not necessarily constitute or imply its endorsement, recommendation, or favoring by the United States Government or any agency thereof, or The Regents of the University of California. The views and opinions of authors expressed herein do not necessarily state or reflect those of the United States Government or any agency thereof, or The Regents of the University of California.

This work was supported by the Director, Office of Science, Office of Basic Energy Sciences, of the U.S. Department of Energy under Contract No. DE-AC02-05CH11231.

Intra-beam scattering for free electron lasers and its modeling in chicanes

G. Penn

Lawrence Berkeley National Laboratory

August 2014

Abstract

Some FEL beamlines, especially those based on echo-enabled harmonic generation (EEHG), are sensitive to small, random jumps in energy generated by incoherent processes such as intra-beam scattering (IBS) and incoherent synchrotron radiation (ISR). Here, we examine the energy jumps caused by IBS when the local energy spread is a negligible factor compared to the transverse momentum spread, as is typical in accelerators. A simulation tool for modeling chicanes incorporating the effect of IBS is described.

1 Introduction

Intrabeam scattering (IBS) is an important effect which can increase the energy spread of a beam without requiring any external interactions. Because of the nature of the echo-enabled harmonic generation (EEHG) scheme [1, 2], it is particularly important to take into account all forms of energy scatter during the beam manipulations, in particular within and in between the two chicanes. The second modulating undulator is therefore as sensitive to scattering as the chicanes themselves [3]. Sources of energy scattering include IBS, incoherent synchrotron radiation (ISR), and neutral gas scattering. In order to reduce ISR, magnetic fields must be kept low in both the chicanes and the second modulating undulator. This tends to increase the length of the chicanes and either the length of the second undulator or the required input laser power. Because IBS occurs everywhere, increasing the length of any element necessarily increases the total impact of IBS.

Here we describe some basic estimations of IBS and present a simple simulation tool, `chicane_ibs`, which models basic transport, ISR, and IBS across a typical 4-dipole chicane. By setting the magnetic field to zero, drifts can be simulated as well. This is to be used in EEHG simulation studies because the built-in `GENESIS` [4] model for chicanes uses a deterministic map for the electrons and scattering is neglected. While `GENESIS` does model ISR in undulators, the effect of IBS is not included. For thorough EEHG simulations, the impact of IBS within an undulator section can be approximated by estimating the total rms

energy offset caused by IBS and applying it at the end of the undulator. This should be a reasonable approximation unless the undulator is much longer than a gain length. More features may be added to future versions of this code.

2 Poisson statistics of Coulomb collisions

The statistics of collisions follows a Poisson distribution, where the standard deviation in the number of collisions is equal to the square root of the average number of collisions. Thus, we have

$$\langle N \rangle = \int \nu dt = \langle (\Delta N)^2 \rangle. \quad (1)$$

This can be viewed as coming from the fact that in each time interval Δt , the fluctuation in collisions is $\sqrt{\nu \Delta t}$, and these fluctuations scale in quadrature. For a given effect Y caused by collisions, we have

$$\langle Y \rangle = \int Y \nu dt, \quad \sigma_Y^2 = \int Y^2 \nu dt. \quad (2)$$

Note that this is different from moments of a distribution function in that there is no normalization to enforce $\langle 1 \rangle = 1$ because this would give the average change per collision, rather than the expectation value of the cumulative effect of many collisions.

For IBS in the case of small energy spreads, we are interested primarily in $Y = v_z$, where v_z is the longitudinal velocity in the rest frame of the electron beam generated by collisions. Clearly $\langle v_z \rangle \equiv 0$, but growth of $\langle v_z^2 \rangle$ is of critical importance when there is fine-scale structure in the longitudinal phase space of the electron beam.

Although there exists one important constraint on two-body collisions, that each collision event affects two electrons in equal and opposite ways, this should have little effect on rms properties of the electron bunch. In particular, even though net momentum must obviously be conserved exactly, it is a good approximation to ignore correlations.

3 Kinematics of Coulomb Collisions

We start by examining collisions in the rest frame of the electron bunch. The basic definition of scattering rate is $\nu = n_e v_{\text{rel}} \sigma$, where v_{rel} is the relative velocity between the two populations that are scattering against each other. All of these quantities are for a given region in space, which is assumed small enough such that the local distribution can be viewed as uniform in space and having some distribution in velocity space. In the rest frame, all velocities should be non-relativistic. The number of collisions for a given set of impact parameters is given by

$$dN = dt P(\vec{v}_{\text{rel}}) d\vec{v}_{\text{rel}} n_e v_{\text{rel}} b db d\phi, \quad (3)$$

where $P(\vec{v}_{\text{rel}})$ is the probability of a random pair of electrons at a particular location having a given relative velocity. Now we will get the greatest simplification by assuming that in

the rest frame, the spread in longitudinal velocities is completely negligible compared to the effect of transverse velocities. With all velocities in the x - y plane, the velocity kick out of this plane is the only aspect of collisions we care about for predicting the spread in longitudinal velocities. Furthermore, as long as everything is nonrelativistic, this component is independent of the orientation of the x and y axes, and is also unchanged by any shift in reference frame involving only v_x or v_y . In particular, the longitudinal kick in the center of momentum (COM) frame of any pair of electrons is identical to the kick in the beam frame (where only $\langle v_z \rangle$ is set to 0). We can choose the orientation of the coordinate system so that the scattering angle is defined by χ and ϕ , and the longitudinal velocity kick

$$\Delta v_z = \frac{1}{2} v_{\text{rel}} \sin \chi \sin \phi. \quad (4)$$

Thus, $\chi = 0$ gives no interaction, $\chi = \pi$ gives full backscatter of the electrons, $\phi = 0$ or $\phi = \pi$ gives collisions that stay within the x - y plane, and $\phi = \pm\pi/2$ gives collisions that scatter most directly towards the $\pm z$ directions. Because the orientation of \vec{v}_{rel} does not affect the longitudinal kicks, we can write the scattering in terms of the probability $P(v_{\text{rel}})$, lumping together all relative velocities having the same magnitude:

$$dN = dt P(v_{\text{rel}}) dv_{\text{rel}} n_e v_{\text{rel}} b db d\phi. \quad (5)$$

The relationship between χ and impact parameter b now needs to be calculated in order to replace this with an integral over scattering angle, which will allow us to calculate the induced spread in v_z . We know by symmetry that the expectation value of v_z must be zero, and in fact the average must always be identically zero by conservation of momentum.

Scattering kinematics can be mostly easily calculated in the COM frame because for each pair of particles, ignoring interference from third particles, the center of mass does not move. The dynamics of the problem can then be isolated by using reduced coordinates $\vec{r} = \vec{r}_1 - \vec{r}_2$. In terms of \vec{r} the potential, $U(r)$, is fixed with its center at the origin. The velocity $\vec{v} = d\vec{r}/dt$ is the instantaneous relative velocity. In this coordinate system the dynamics is equivalent to a single particle with reduced mass $\mu = m_1 m_2 / (m_1 + m_2)$ in a fixed potential U , as if generated by a stationary object at the origin. For electrostatic interactions between electrons, $\mu = m_e/2$ and $U(r) = e^2/4\pi\epsilon_0 r$. The force in this frame becomes

$$\vec{F} = \frac{e^2}{4\pi\epsilon_0 r^2} \frac{\vec{r}}{r}, \quad (6)$$

where r is the distance between the two electrons. The total energy

$$E_T = \frac{1}{2} \mu v^2 + U(r) = \frac{1}{2} \mu (\dot{r}^2 + r^2 \dot{\theta}^2) + U(r) = \frac{1}{2} m_1 v_1^2 + \frac{1}{2} m_2 v_2^2 + U(r), \quad (7)$$

and is equal to $\mu v_{\text{rel}}^2/2$. The total angular momentum is $\vec{L}_T = \mu \vec{r} \times \vec{v} = \mu r^2 \dot{\theta} = m_1 \vec{r}_1 \times \vec{v}_1 + m_2 \vec{r}_2 \times \vec{v}_2$ is constant and has magnitude $\mu b v_{\text{rel}}$, where b is the impact parameter and v_{rel} is the velocity as $t \rightarrow -\infty$.

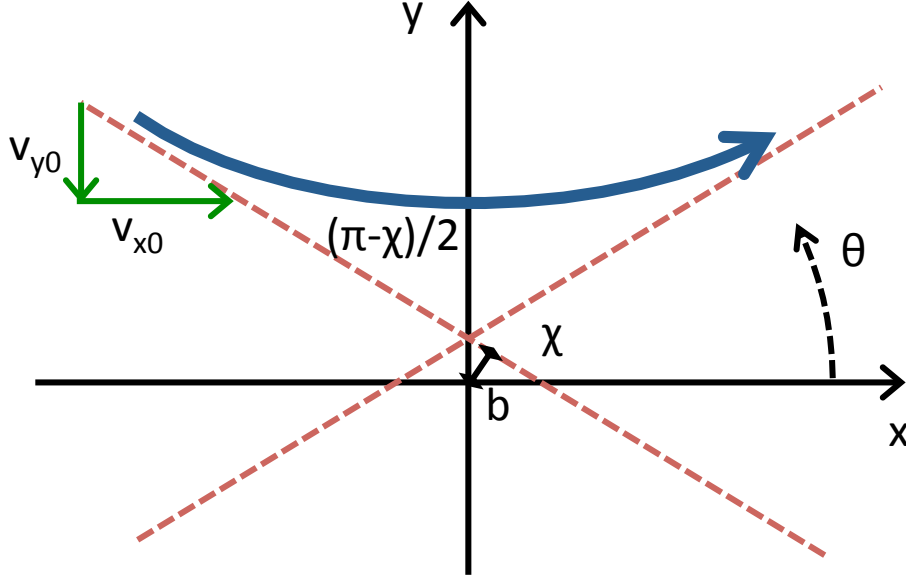


Figure 1: Alignment of scattering process for simple calculation of relationship between χ and impact parameter.

While the initial $t \rightarrow -\infty$ relative velocity is assumed to lie in the x - y plane, the paths lies in a plane defined by the incoming velocities, which are parallel to each other in the COM frame, and the scattering angle or equivalently the orientation of the impact parameter. One trick for quickly calculating the resulting scattering angle is to reorient the coordinates so that the trajectories of the electrons lie within a new x - y plane and are symmetric about $x = 0$, as in Fig. 1, and to note that for the incoming and outgoing ends of the trajectory the horizontal components of velocity must be identical, while the vertical components of velocity must be equal and opposite. Thus, the integral of the vertical force over time must be just enough to flip the vertical velocity. For scattering angle χ , the “vertical” relative velocity must be $\pm v_{\text{rel}} \cos[(\pi - \chi)/2]$. From the vertical force equation,

$$F_y = \frac{dP_y}{dt} = \frac{e^2}{4\pi\epsilon_0 r^2} \cos \theta, \quad (8)$$

and integrating over all time yields

$$\begin{aligned} \Delta P_y &= 2\mu v_{\text{rel}} \cos\left(\frac{\pi - \chi}{2}\right) = 2\mu v_{\text{rel}} \sin(\chi/2) \\ &= \int dt \frac{e^2}{4\pi\epsilon_0 r^2} \cos \theta = \int d\theta \frac{\mu e^2}{4\pi\epsilon_0 L_T} \cos \theta = \frac{\mu e^2}{4\pi\epsilon_0 L_T} \sin \theta \Big|_{-(\pi-\chi)/2}^{(\pi-\chi)/2} = \frac{\mu e^2}{2\pi\epsilon_0 L_T} \cos(\chi/2). \end{aligned} \quad (9)$$

Using $L_T = \mu b v_{\text{rel}}$ and $\mu = m_e/2$, we obtain

$$\tan \frac{\chi}{2} = \frac{b_{90}}{b}, \quad (10)$$

where

$$b_{90} \equiv \frac{e^2}{2\pi\epsilon_0 m_e v_{\text{rel}}^2} \quad (11)$$

is the impact parameter which yields a 90 degree scattering angle. In terms of more general particle combinations, the result is the same but $b_{90} = q_1 q_2 / (4\pi\epsilon_0 \mu v_{\text{rel}}^2)$.

We can also solve the particle trajectory directly from Eq. (7) and using $\dot{\theta} = L_T / (\mu r^2) = b v_{\text{rel}} / r^2$, yielding

$$\frac{dr}{d\theta} = \text{sgn}(\dot{r}) \frac{r}{b v_{\text{rel}}} \sqrt{r^2 \frac{4E_T}{m_e} - r \frac{e^2}{\pi\epsilon_0 m_e} - b^2 v_{\text{rel}}^2}. \quad (12)$$

Noting that $E_T = m_e v_{\text{rel}}^2 / 4$, the general solution is

$$\tan(\theta - \theta_0) = \text{sgn}(\dot{r}) \frac{b v_{\text{rel}}}{(e^2 / 2\pi\epsilon_0 m_e) r + b^2 v_{\text{rel}}^2} \sqrt{r^2 v_{\text{rel}}^2 - \frac{e^2}{\pi\epsilon_0 m_e} r - b^2 v_{\text{rel}}^2}. \quad (13)$$

As $r \rightarrow \infty$, this yields

$$\theta = \theta_0 \pm \arctan\left(\frac{4\pi\epsilon_0 m_e b v_{\text{rel}}^2}{e^2}\right) = \theta_0 \pm \arctan\left(\frac{b}{b_{90}}\right), \quad (14)$$

consistent with the earlier calculation because the total change in θ is $\pi - \chi$.

4 Eliminating the Impact Parameter

Now that we have the change in angle from any scattering event in terms of Eq. (10), we can substitute this into the scattering probability. From

$$\frac{db}{d\chi} = -\frac{1}{2} b_{90} \csc^2\left(\frac{\chi}{2}\right), \quad (15)$$

we find

$$dN = dt P(v_{\text{rel}}) dv_{\text{rel}} n_e v_{\text{rel}} \frac{1}{4} b_{90}^2(v_{\text{rel}}) \frac{\sin \chi}{\sin^4(\chi/2)} d\chi d\phi. \quad (16)$$

To obtain the induced spread in longitudinal velocities, we multiply by v_z^2 and integrate over time and v_{rel} , over χ between 0 and π , and over ϕ between 0 and 2π ,

$$\langle \Delta v_z^2 \rangle = \Delta t \int dv_{\text{rel}} P(v_{\text{rel}}) n_e \frac{1}{16} v_{\text{rel}}^3 b_{90}^2(v_{\text{rel}}) \int_0^{2\pi} d\phi \sin^2 \phi \int_0^\pi d\chi \frac{\sin^3 \chi}{\sin^4(\chi/2)}. \quad (17)$$

Again, note that there is no need for further normalization, either to the number of collisions or particles, because this is the statistical result for all of the collisions a single electron will undergo in a given time interval. The ϕ integral is trivial and just yields a factor of π . The χ integral is divergent, with general solution $16 \ln[\sin(\chi/2)] - 8 \sin^2(\chi/2)$. Instead of taking

the integral from $\chi = 0$ to $\chi = \pi$, we will impose a cutoff for small angles by limiting the corresponding impact parameter b to values less than a Debye length λ_D , where

$$\lambda_D = \left(\frac{\epsilon_0 kT}{n_e e^2} \right)^{1/2}. \quad (18)$$

Here we will be approximate and just take the typical perpendicular temperature, since the main result will depend on a logarithm. The corresponding minimum χ is about $2b_{90}/\lambda_D$, and we will ignore variation with v_{rel} and just approximate the relative velocity as $2\sqrt{kT/m_e} = 2\sigma_v$, fitting the velocity distribution to a Gaussian. Then $b_{90} \approx 1/(8\pi n_e \lambda_D^2)$ and the minimum χ is roughly $1/(4\pi n_e \lambda_D^3)$. Taking advantage of the fact that χ_{min} is very small, the integral over χ then can be approximated as $16[\ln(2/\chi_{\text{min}}) - 1/2]$. The $1/2$ term is usually ignored because the calculation does not have that level of accuracy anyway (and it is only good for large values of the logarithm), and we write this as $16 \ln(8\pi n_e \lambda_D^3)$. More often, still keeping to an order unity accuracy, the argument of the logarithm is taken to be the plasma parameter $\Lambda = (4\pi/3)n_e \lambda_D^3$, which is the number of electrons in a sphere with radius λ_D . This gives us

$$\langle \Delta v_z^2 \rangle \simeq \Delta t 4\pi \ln \Lambda n_e r_e^2 c^4 \int dv_{\text{rel}} \frac{P(v_{\text{rel}})}{v_{\text{rel}}}, \quad (19)$$

where $r_e = e^2/(4\pi\epsilon_0 m_e c^2)$. The distribution of kicks in v_z is not Gaussian for large kicks, and we will revisit the logarithm term in a later section to only capture the small-angle collisions which are relevant to smearing out the longitudinal phase space. Electrons which receive more than a certain kick will be treated like losses instead.

5 Relative velocity distribution

By ignoring initial longitudinal velocities in the rest frame, we simplify the calculation so that the effect of scattering is a simple integral over the local distribution of relative velocities. This distribution is quite trivial in the case where the horizontal and vertical velocities have equal spreads, with

$$P(v_{\text{rel}}) = \frac{v_{\text{rel}}}{2\sigma_v^2} e^{-v_{\text{rel}}^2/4\sigma_v^2}. \quad (20)$$

Note that the velocity distribution is correlated with transverse position through the Courant-Snyder parameters α_x and α_y . However, we shall see below that the Debye length can be comparable to the transverse size of the electron bunch. Because the scattering rate increases as the velocity spread decreases, we take a conservative approach of using the smaller, local velocity spread $\sigma_v/c = \epsilon_N/\beta\gamma$. The integral of P/v_{rel} then becomes $\sqrt{\pi}/2\sigma_v$.

For an asymmetric beam, the probability becomes

$$P(v_{\text{rel}}) = \frac{v_{\text{rel}}}{2\sigma_{vx}\sigma_{vy}} e^{-v_{\text{rel}}^2/8\sigma_{vx}^2} e^{-v_{\text{rel}}^2/8\sigma_{vy}^2} I_0 \left[\frac{v_{\text{rel}}^2}{8} \left(\frac{\sigma_{vx}^2 - \sigma_{vy}^2}{\sigma_{vx}^2 \sigma_{vy}^2} \right) \right], \quad (21)$$

where I_0 is the modified Bessel function of the first kind. The integral of P/v_{rel} can be expressed in terms of the complete elliptic integral K as

$$\int dv_{\text{rel}} \frac{P(v_{\text{rel}})}{v_{\text{rel}}} = \frac{1}{\sigma_{vx}\sqrt{\pi}} K \left(\sqrt{1 - \frac{\sigma_{vy}^2}{\sigma_{vx}^2}} \right) = \frac{1}{\sqrt{\pi}} \frac{2}{\sigma_{vx} + \sigma_{vy}} K \left(\frac{\sigma_{vx} - \sigma_{vy}}{\sigma_{vx} + \sigma_{vy}} \right). \quad (22)$$

Note that the integral is simpler to calculate without using $P(v_{\text{rel}})$ as an intermediate step, because the distribution function has elliptical contours. The complete elliptic integral is related to the arithmetic-geometric mean, which is here denoted as $M(x, y)$ and is defined by $M(x, y) = M[(x + y)/2, \sqrt{xy}]$, which quickly converges by iteration to equal arguments. We can use the identity

$$K \left(\frac{x - y}{x + y} \right) = \frac{\pi}{4} (x + y) \frac{1}{M(x, y)} \quad (23)$$

and use the definition of M to apply a rough approximation

$$M(x, y) \simeq \left[\left(\frac{x + y}{2} \right) \sqrt{xy} \right]^{1/2}. \quad (24)$$

Unless the ratio σ_{vx}/σ_{vy} is either very large or very small, this should be correct to within a few percent. Our final expression for the net change in the local spread of velocities is

$$\langle \Delta v_z^2 \rangle \simeq \Delta t 2\pi^{3/2} \ln \Lambda n_e r_e^2 c^4 \left(\frac{\sigma_{vx} + \sigma_{vy}}{2} \sqrt{\sigma_{vx}\sigma_{vy}} \right)^{-1/2}. \quad (25)$$

In the symmetric case the last term is simply $1/\sigma_v$.

6 Scattering in the lab frame

Here we will continue to denote rest frame properties as above, and explicitly denote quantities in the lab frame with a superscript. The transformation is taken to be a boost in the z -direction with velocity u_b , and corresponding $\gamma_b = 1/\sqrt{1 - u_b^2/c^2}$.

In the lab frame, due to Lorentz contraction and time dilation, the density is related to that of the rest frame by $n_e^{\text{lab}} = \gamma_b n_e$, and the elapsed time is $\Delta t^{\text{lab}} = \gamma_b \Delta t$. Also, for a longitudinal velocity v_z which is much smaller than u_b , the deviation in longitudinal momentum in the lab frame is simply $m_e \delta(\gamma^{\text{lab}} v_z^{\text{lab}}) \simeq m_e \gamma_b v_z$. The transverse momentum is unchanged by the change in reference frame, and it can be approximated by $m_e \gamma_b v_{\perp}^{\text{lab}}$. Thus, we can approximate $v_{\perp}^{\text{lab}} \simeq v_{\perp}/\gamma_b$, and $\sigma_v^{\text{lab}} \simeq \sigma_v/\gamma_b$. For large γ_b , the relative energy shift from a collision is roughly equal to v_z/c , so the induced energy spread in the lab frame becomes

$$\langle (\Delta \gamma^{\text{lab}})^2 \rangle \simeq \frac{\gamma_b^2}{c^2} \langle \Delta v_z^2 \rangle. \quad (26)$$

Finally, we can replace the time elapsed in the lab frame with $\Delta s \simeq c \Delta t^{\text{lab}}$. Thus, the effect of scattering on the energy spread in the beam is

$$\langle (\Delta \gamma^{\text{lab}})^2 \rangle \simeq \Delta s 2\pi^{3/2} \ln \Lambda r_e^2 c n_e^{\text{lab}} \frac{1}{\sigma_v^{\text{lab}} \gamma_b} \simeq \Delta s 2\pi^{3/2} \ln \Lambda r_e^2 n_e^{\text{lab}} \frac{1}{\sigma_{\theta}^{\text{lab}} \gamma_b}. \quad (27)$$

The Coulomb logarithm still has to be calculated in terms of rest frame parameters. The plasma parameter is

$$\begin{aligned}\Lambda &= \frac{4\pi}{3} n_e \lambda_D^3 = \frac{4\pi}{3} (4\pi r_e)^{-3/2} \left(\frac{\sigma_v}{c}\right)^3 n_e^{-1/2} = \frac{\sqrt{2}}{6} \frac{\sigma_x}{r_e} \left(\frac{\sigma_v^{\text{lab}}}{c}\right)^3 \left(\frac{I}{I_A}\right)^{-1/2} \gamma_b^{7/2} \\ &= \frac{\sqrt{2}}{6} \frac{\epsilon_N^3}{r_e \sigma_x^2} \left(\frac{I}{I_A}\right)^{-1/2} \gamma_b^{1/2}.\end{aligned}\quad (28)$$

The above expression tends to over-estimate the impact of IBS in an FEL because large-angle scatters, though rare, do not quite fit the Gaussian dependence and significantly increase the standard deviation. It would be more appropriate to calculate the scattering that fits within the bandwidth of the FEL, or even within the typical slice energy spread, and then treat all electrons with larger energy shifts as being effectively lost. This can reduce the effective logarithm, while the effective losses are miniscule because they correspond to very small values of the impact parameter. Even so, typically the scattering angle at this cutoff will be small compared to unity. The fractional losses are given by $f = \Delta t \pi^{3/2} n_e \sigma_v b_{\min}^2$, where $b_{\min} \simeq 2b_{90} \sigma_v / c\eta$, and η is taken to be the allowed relative energy shift. The FEL bandwidth is a reasonable value to take for η . The logarithm will be reduced by subtracting out $\ln 2\sigma_v / \eta c = \ln 2\epsilon_N / \eta \sigma_x$. The relative size of the correction tends to be modest. For other applications, such as estimating the Touschek effect, using such a cutoff is probably not appropriate.

This result gives the scattering rate averaged over all electrons at a given location. In order to get a more detailed picture, we can focus on the rate for one electron with a given velocity. Assuming axisymmetry around the average trajectory, we can just consider the magnitude of the difference between the electron velocity and the average velocity, which we will denote simply as v_{\perp} . This is distributed according to

$$F(v_{\perp}) = \frac{v_{\perp}}{\sigma_v^2} e^{-v_{\perp}^2 / 2\sigma_v^2}.\quad (29)$$

The distribution of relative velocities between that electron and nearby electrons is given by

$$P(v_{\text{rel}}; v_{\perp}) = \frac{v_{\text{rel}}}{\sigma_v^2} e^{-v_{\perp}^2 / 2\sigma_v^2} e^{-v_{\text{rel}}^2 / 2\sigma_v^2} I_0\left(\frac{v_{\perp} v_{\text{rel}}}{\sigma_v^2}\right).\quad (30)$$

The required integral is still

$$\int dv_{\text{rel}} \frac{P(v_{\text{rel}}; v_{\perp})}{v_{\text{rel}}} = \frac{1}{\sigma_v} \left(\frac{\pi}{2}\right)^{1/2} e^{-v_{\perp}^2 / 4\sigma_v^2} I_0\left(\frac{v_{\perp}^2}{4\sigma_v^2}\right).\quad (31)$$

If we average this over the weighting $F(v_{\perp})$ we will obtain our original result. The difference between the velocity-specific result and the average is given by the factor

$$G(v_{\perp}) = \sqrt{2} e^{-v_{\perp}^2 / 4\sigma_v^2} I_0\left(\frac{v_{\perp}^2}{4\sigma_v^2}\right) \approx \left(\frac{1}{\sqrt{2}} + \frac{\sqrt{\pi x}}{1 + 1/x}\right)^{-1},\quad (32)$$

where the last expression is a reasonable approximation in terms of simple functions and where $x = (v_{\perp}/2\sigma_v)^2$. The behavior of this function is that it goes to a maximum of $\sqrt{2}$ at small velocities, equals unity at $v_{\perp} \simeq 1.2\sigma_v$, and decreases as $(2/\sqrt{\pi})\sigma_v/v_{\perp}$ for $v_{\perp} \gg \sigma_v$. Thus, for the electrons with the lowest offset in transverse velocity, the energy diffusion rate is increased by a factor of up to $\sqrt{2}$. The tail of the velocity distribution actually suffers less scattering, because those electrons will have a large relative velocity relative to the majority of the neighboring electrons.

7 Lab frame dynamics

Here we will use the above results to explore behavior exclusively in the lab frame, and will drop all superscripts. Assuming no dispersion, the local density is

$$n_e = \frac{I}{I_A} \frac{1}{2\pi r_e \sigma_x \sigma_y} e^{-x^2/2\sigma_x^2} e^{-y^2/2\sigma_y^2}, \quad (33)$$

where the Alfvén current $I_A = ec/r_e \simeq 17.05$ kA. Taking into account the local average angle, the local spread in angles is $\sigma_{\theta x} = \sigma_x/\beta_x$, $\sigma_{\theta y} = \sigma_y/\beta_y$. Taking a symmetric beam,

$$\langle \Delta\gamma^2 \rangle \simeq \Delta s 2\pi^{3/2} \ln \Lambda r_e \frac{I}{I_A} \frac{1}{2\pi\sigma_x^3} e^{-r^2/2\sigma_x^2} \frac{\beta_x}{\gamma_b} \simeq \Delta s \pi^{1/2} \ln \Lambda r_e \frac{I}{I_A} e^{-r^2/2\sigma_x^2} \frac{1}{\sigma_x \epsilon_N}. \quad (34)$$

Assuming a Gaussian current profile with maximum current I_0 , we can write this in terms of the total number of electrons, N_e , as

$$\langle \Delta\gamma^2 \rangle \simeq \Delta s N_e 2^{-1/2} \ln \Lambda r_e^2 e^{-z^2/2\sigma_z^2} e^{-r^2/2\sigma_x^2} \frac{1}{\sigma_z \sigma_x \epsilon_N}. \quad (35)$$

To compare this result with other calculations, first we must average over all electrons in the bunch. This makes more sense for a typical ring where synchrotron and betatron motion mixes all electrons in the bunch, but is not so useful for our purposes. The result is $\langle \Delta\gamma^2 \rangle = \Delta s N_e \ln \Lambda r_e^2 / (4\sigma_z \sigma_x \epsilon_N)$, which agrees with Ref. [5]. For an actual ring evaluation, the energy scatter turns into a longitudinal phase space growth, with half of the energy scatter going into increasing the bunch length in order to preserve the matching to longitudinal bucket, which yields an additional factor of 1/2. This result agrees with Ref. [6, 7] in the limit where there is transverse symmetry and the rest frame spread in longitudinal velocities is small compared to that of transverse velocities.

The dependence on density is unfortunate because particles on axis will undergo larger energy jumps, but this is the most desirable place to preserve bunching. It is also apparent that electrons with the smallest transverse amplitudes (and thus small angles) also undergo IBS at a slightly higher rate than high-amplitude particles with big angles.

8 A numerical example

We consider parameters for LCLS-II[8] for a bunch charge of 300 pC. The electron beam parameters are 4 GeV energy, 0.43 micron emittance, 1 kA peak current, 500 keV energy

spread, and 15 m beta function. The typical beam radius is 29 micron, the rms bunch length is roughly 12 micron, and the typical transverse momentum is $0.015 m_e c$. In the rest frame, the transverse velocity spread is $0.015 c$, the longitudinal velocity spread $1.25 \times 10^{-4} c$, and the Debye length is 110 micron. In the lab frame the Debye length is unchanged in the transverse direction, while in the longitudinal direction it transforms to 14 nm.

The Coulomb logarithm $\ln \Lambda = 14.9$. However, we are in a parameter regime where the transverse size is significantly less than a Debye length, so it makes sense to restrict the maximum impact parameter to be not more than the transverse size, which changes the argument of the logarithm to

$$\Lambda = \frac{4\pi}{3} n_e \lambda_D^2 \sigma_x . \quad (36)$$

This changes the logarithm to be 13.5. If we go further and take the total number of electrons within $\pm \lambda_D$ of a test particle in the rest frame, that yields $\Lambda = 2\lambda_D I / ec$ and the logarithm is slightly reduced to 13.3. However, this is not standard practice and may be misleading in some circumstances.

For an FEL bandwidth of 10^{-3} , we can take $\eta = 0.001$ which multiplies the argument of the logarithm by a factor (in the rest frame) $\eta c / 2\sigma_v \simeq 0.033$. This is equivalent to subtracting 3.4 from the logarithm, yielding a factor close to 10. These details have a moderate impact but may have practical implications. The nominal intrabeam scattering rate, forcing the maximum impact to be below σ_x and the maximum relative energy shift to be below 10^{-3} , is $(5.6 \text{ keV})^2$ per meter (note that this is a diffusion process).

The Debye length in the lab frame is an interesting parameter for undulators. If an undulator is tuned to be in resonance to a wavelength shorter than λ_D / γ , here equal to 14 nm, then slices of the electron beam which are kicked in opposite directions will be less than a Debye length apart and intrabeam scattering will be damped by the large velocity differential. There are a mix of effects because the overall Lorentz factor for the beam is reduced to be $\gamma_z \equiv \gamma / (1 + K^2 / 2)$ (for a planar undulator) where $K = eB_0 / mck_u$ is the peak undulator parameter. Meanwhile, the undulator imparts a transverse momentum as large as $p_\perp = Km_e c$. For a modest $K = 1$, this gives a transverse momentum which oscillates between $\pm m_e c$ which is much larger than the thermal velocity spread of $0.015 m_e c$. The transverse motion in the rest frame is relativistic and the previous calculations will not be accurate. Even if we only consider longitudinal separations of the same order as σ_x / γ_z , this gives a minimum wavelength of 5.5 nm below which variations in transverse velocity with longitudinal position have to be taken into account.

9 Code for modeling chicanes

Here we present a code, `chicane_ibs`, which transports a beam through a symmetric chicane defined by four dipoles while applying scatter due to IBS and ISR. Equal drifts at the beginning and end of the chicane are allowed. ISR is included as well. It is written in Fortran. Wakefields and scattering off of neutrals are not considered at all, but they could be added. The code reads in the particle dump format from GENESIS and outputs the

particle distribution at the end of the chicane in the same format. This particle format bins the macroparticle distribution into distinct slices, but temporal information can be extracted from a combination of the slice number and the particle phase. A reference particle originally on axis and with a given energy is used to define a reference phase. The slice-by-slice current has to be defined through an external file, in a similar way as how **GENESIS** is run, to vary the IBS scattering rate from slice to slice. Note that the slice separation may be smaller than the Debye length. In general, the actual scatter of individual macroparticles are completely uncorrelated; there are no pairwise scattering events. Even without ISR, energy is conserved only in terms of expectation values.

The inner and outer dipole pairs may be different in both length and magnetic field, but in practice they are chosen to be identical. There is no adjustment to compensate for the energy loss in the bend. For chicanes used in an FEL beamline this should be of no consequence. The dipoles are assumed to be rectangular rather than sector dipoles. By setting the magnetic field to zero, the dynamics are those of a drift. The rates of ISR may be scaled by an input parameter, and the average and fluctuating parts are scaled separately. Because the value of the Coulomb logarithm is an input parameter, this serves as a scaling parameter as well. IBS has three models: it can be turned off completely, or the expectation value of the energy scatter for each particle can be set to the average, so that every particle has the same scattering probability, or the scattering can be made proportional to the local density. A future version of the code will include different scattering probabilities based on the relative velocity of each electron relative to that of the local slice.

Electrons are tracked spatially rather than in time. There are three basic elements: a drift, an uniform dipole field, and a thin fringe field. The thin fringe field simply applies transverse focusing. The drift and dipole elements are each divided into a fixed number of equal parts; at the end of each subdivision, the expected energy deviations from IBS and ISR (for dipoles) are applied. The number of steps taken in each element is a free parameter (typically 4 steps are used).

Initial beta and alpha functions are set as input parameters; these are then tracked step by step to calculate the local IBS scattering rate. The input beam properties are not used to calculate these parameters self-consistently in the present version of the code. In particular, any change in local density due to dispersion is ignored. The evaluation of IBS uses the approximation of Eq. 24 to calculate the elliptic function.

The key components of the tracking are given below. For the fringe fields, taken to be arbitrarily short:

```
do i=1,npart
  pz=dsqrt(gamma(i)**2-1.d0-px(i)**2-py(i)**2)
  phi=emc*deltaBy*y(i)/pz
  pxt=px(i)
  pyt=py(i)
  px(i)=pxt*dcos(phi)-pyt*dsin(phi)
  py(i)=pxt*dsin(phi)+pyt*dcos(phi)
end do
```

In general, the peak IBS scattering rate is calculated from combining Eqs. 22 through 24,

```

    ibsgam0=dsqrt(length*scalecurrent/
&    (sigma(1)*sigma(2)*
&    dsqrt((sigmapperp(1)+sigmapperp(2))/2*
&    dsqrt(sigmapperp(1)*sigmapperp(2))))

```

and it is then either divided by 2 to get the average, or multiplied by the normalized local electron density. Within each of segment of the dipole field, the transport is calculated by assuming motion in an arc of a circle given by the Larmor radius, or equivalently by conserving canonical momentum. The scattering for each particle from ISR is also calculated based on the field and the path length.

```

    invrho=emc*By/gamma(i)
    ps=dsqrt(pzi**2+px(i)**2)
    pxf=px(i)+emc*By*length
    pzf=dsqrt(pzi**2+px(i)**2-pxf**2)
    cdeltat=gamma(i)/(emc*By)*(dasin(pxf/ps)-dasin(px(i)/ps))
    dgam=-(2.d0/3.d0)*relcl*gamma(i)**4*invrho**2*cdeltat
    sgam=dsqrt((55.d0/24.d0/dsqrt(3.d0))*(relcl**2/alphac)*
&    gamma(i)**7*dabs(invrho)**3*cdeltat)
    delta_gam=scale_avg*dgam+scale_sig*gasran(ran_seed)*sgam
    x(i)=x(i)+(pzi-pzf)/(emc*By)
    y(i)=y(i)+cdeltat*py(i)/gamma(i)
    th(i)=th(i)-(2*pi/xlamds)*(cdeltat-cdeltat_ref)

```

The combined energy scatter from ISR and IBS is applied at the end of each segment, with an additional constraint that the vertical velocity and the angles in the $x - z$ plane are conserved. This makes more sense for ISR but is not unreasonable for IBS, especially because only changes in the energy are being applied and we are ignoring changes in transverse momentum due to IBS.

```

c  conserve v_y and final px/pz
    px(i)=pxf*dsqrt((1.d0+ps**2)*gamf**2/gami**2-1.d0)/ps
    py(i)=py(i)*gamf/gami

```

Reference particle and beam lattice parameters are also updated going through each segment, both for relative phase information and to compute local density functions. The drift calculations are a simplification of those for the uniform magnetic field.

An example input file for LCLS-II would be:

```

und1.out.dpa    ! particle input file
chicane1.dpa    ! particle file at end of chicane
260.E-09        ! radiation wavelength (m) [defines theta]
540000          ! npart

```

```

1           ! number of slices
7828.81    ! reference gamma
0.25      ! drift length 1
2.00      ! magnet length 1
0.3938    ! magnet field 1
0.25      ! drift length 2
2.00      ! magnet length 2
0.25      ! drift length 3 (rest is mirror symmetric)
1.0       ! scales average energy loss due to ISR
1.0       ! scales energy spread due to ISR
4         ! number of times to calculate ISR and IBS per element
-11       ! random number seed
1         ! ibs model (0=off, 1=uniform, 2=indep of velocity)
0.43e-6 0.43e-6 ! X & Y emittances
15. 15.   ! X & Y initial beta
1.  -1.   ! X & Y initial alpha
10        ! Coulomb logarithm value (treated as free parameter)
current.txt ! name of file for slice current information

```

10 Simulation example and code comparison

We consider a time-independent simulation of the nominal LCLS-II parameters to use two modulations with a wavelength of 260 nm in order to reach a wavelength of 1 nm. The first undulator has a period of 0.1 m and a total length of 3.4 m. An external laser with 47 MW of power yields an energy modulation of 1.5 MeV. This is followed by a 9-m long chicane with $R_{56} = 11.03$ mm. The next undulator has a period of 0.4 m (to keep the magnetic field below 0.5 T) and a total length of 3.4 m. The second laser requires a power of 400 MW to yield an energy modulation of 2 MeV. The second chicane is about 2 m long and has $R_{56} = 103 \mu\text{m}$. This is followed by a series of 39-mm period undulators which radiate at 2 nm.

Time-dependent simulations for this beam going from 260 nm external lasers to produce bunching at 2 nm have been performed for various chicane models: using `chicane_ibs` with both IBS and ISR, only with ISR, or without any scatter at all is compared to using `GENESIS` to model the chicanes. Note that although `GENESIS` includes ISR in the undulators, it is not modeled within the chicane. The vertical focusing produced in the chicanes is indistinguishable in all cases, as seen in Fig. 2. Also shown is a horizontal displacement of the order of 1 micron caused by ISR in the chicanes, because after losing energy in the first set of dipoles, the beam is bent back too far in the second set of dipoles. The beam loses 25 keV in the first chicane due to ISR. Although IBS does not change the average energy of the bunch, there does appear to be a second order effect which adds slightly to the bunch displacement. Most importantly, scatter reduces the bunching parameter at the start of the

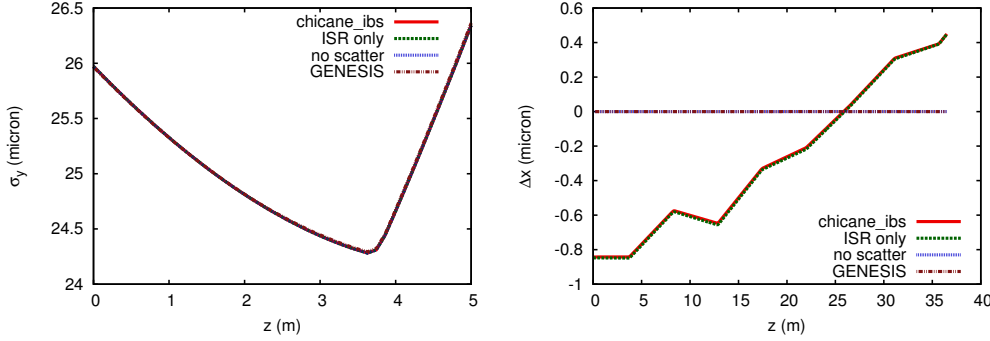


Figure 2: Vertical spot size (left) and horizontal displacement (right) in the section radiating at 2 nm. The `chicane_ibs` models with both IBS and ISR, ISR only, and no scattering are compared to modeling the chicanes using `GENESIS`.

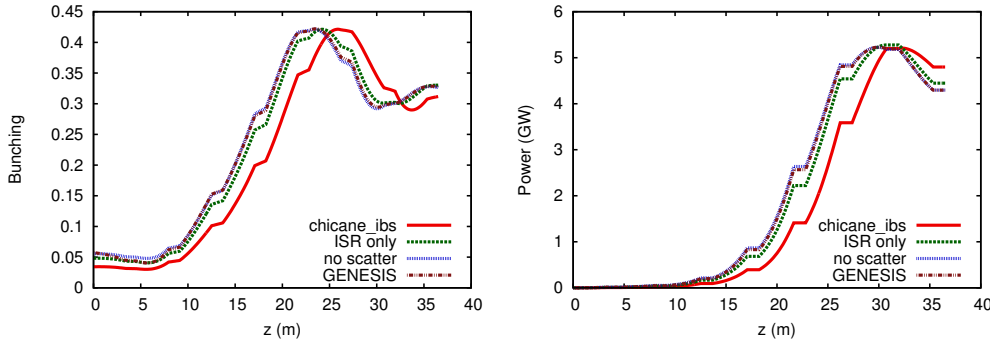


Figure 3: Bunching (left) and power (right) at 2 nm. The `chicane_ibs` models with both IBS and ISR, ISR only, and no scattering is compared to modeling the chicanes using `GENESIS`.

radiation stage, and delays the onset of saturation as seen in Fig. 3.

While the impact of IBS shows up as being stronger than that of ISR, that is an artifact of optimizing the beamline due to the way the scattering terms scale. The scattering rate due to IBS is roughly constant while ISR has a strong power-law dependence on the peak magnetic field; the optimal condition is thus to make the impact of ISR much smaller than that of IBS, because any further reduction of beamline length by increasing the dipole fields will have an oversized impact on the rate of ISR. Similarly, it may appear that ignoring scattering, while overly optimistic, is not disastrous. However, all of the beamline parameters were chosen to minimize the impact of scattering on the beam. Of particular importance are the 2 m length of the individual dipoles in the first chicane to keep the magnetic field below 0.5 T, the long undulator period in the second chicane, and the magnitude of the second energy modulation which was set to 2 MeV. These conditions are all forced by the need to reduce scattering and, in the case of the energy modulation, its impact.

The initial bunching in the cases with scattering turned completely off, including ISR in the second undulator, is 0.059. ISR only in the second undulator, as can be modeled

using GENESIS only, yields a bunching parameter of 0.057. With ISR modeled fully but neglecting IBS, this decreases to 0.048, and IBS reduces this further to 0.034. Without adding additional energy scatter from IBS in the second undulator, the bunching parameter would be 0.041. This is broadly consistent with analytical calculations, taking into account the fact that while the average beta function is 15 m within the final set of undulators, it is somewhat larger in the chicanes.

Appendix: Useful integrals

Some formulas and integrals that are useful for the above detailed calculations are here included. Many are redundant in the sense that we are solving integrals over both v_{rel} and χ , or sometimes v_{rel} and v_{\perp} , and choosing to leave the v_{rel} integral for last. While reversing the order of integration leads to a much simpler calculation, we would miss the physical insight that the distribution over relative velocities can be separated from the general two-body collision problem. It is easier to verify Eq. (13) than to derive it.

$$\int_0^{\infty} dx I_0(x^2) e^{-ax^2} = \frac{1}{\sqrt{\pi(1+a)}} K\left(\sqrt{\frac{2}{1+a}}\right) \quad \{a > 1\}, \quad (37)$$

$$\int_0^{\infty} dx I_0(x^2) e^{-ax} = \frac{1}{\sqrt{a^2-1}} \quad \{a > 1\}, \quad (38)$$

$$\int_0^{\infty} dx I_0(ax) e^{-x^2/2} = \sqrt{\frac{\pi}{2}} e^{a^2/4} I_0\left(\frac{a^2}{4}\right) \quad \{a > 1\}, \quad (39)$$

$$\int_{-1}^1 du \frac{1}{\sqrt{1-u^2}} e^{au} = \pi I_0(a), \quad (40)$$

$$\int_{-1}^1 du \frac{1}{\sqrt{1-u^2}} e^{au^2} = \pi e^{a/2} I_0\left(\frac{a}{2}\right). \quad (41)$$

$$\int \frac{2\sqrt{\lambda}(1-a) d\lambda}{(1+\lambda)^{3/2}(a+\lambda)^2} = \frac{2}{1-a} \left[\frac{2a+1}{\sqrt{a(1-a)}} \tan^{-1}\left(\sqrt{\frac{1-a}{a}} \frac{\lambda}{\lambda+1}\right) - \frac{\lambda}{\lambda+1} \frac{3\lambda+2a+1}{\lambda+a} \right]. \quad (42)$$

Evaluating the above integral from 0 to ∞ yields

$$G(a) = \frac{2}{1-a} \left[\frac{2a+1}{\sqrt{a(1-a)}} \tan^{-1}\left(\sqrt{\frac{1-a}{a}}\right) - 3 \right], \quad (43)$$

which has the limiting forms

$$\begin{aligned} A(a) &\simeq \frac{\pi}{\sqrt{a}} - 8 + \frac{7\pi}{2}\sqrt{a} + O(a) \quad \{a \ll 1\}, \\ &\simeq \frac{8}{15}(1-a) + \frac{41}{35}(1-a)^2 + O((1-a)^3) \quad \{(1-a) \ll 1\}. \end{aligned} \quad (44)$$

References

- [1] G. Stupakov. Using the beam-echo effect for generation of short-wavelength radiation. *Phys. Rev. Lett.*, 102:074801, 2009.
- [2] D. Xiang and G. Stupakov. Echo-enabled harmonic generation free electron laser. *Phys. Rev. ST Accel. Beams*, 12:030702, 2009.
- [3] G. Penn. EEHG performance and scaling laws. LBNL Report LBNL-6481E and NGLS Technical Note 35, LBNL, 10 2013.
- [4] S. Reiche. GENESIS 1.3: a fully 3D time-dependent FEL simulation code. *Nucl. Instr. Meth. A*, 429:243–248, 1999.
- [5] Z. Huang. Intrabeam scattering in an x-ray FEL driver. Report LCLS-TN-02-8, SLAC, 11 2002.
- [6] K.L.F. Bane. A simplified model of intrabeam scattering. In *Proc. European Particle Accelerator Conference 2002*, pages 1443–1445, Paris, France, 2002. JACoW. WEPRI120.
- [7] K. Kubo, S.K. Mtingwa, and A. Wolski. Intrabeam scattering formulas for high energy beams. *Phys. Rev. ST Accel. Beams*, 8:081001, 2005.
- [8] LCLS-II Design Study Group. LCLS-II conceptual design report. Report LCLSII-1.1-DR-0001-R0, SLAC, January 2014.